ELSEVIER

Thermochimica Acta 304/305 (1997) 171–178

thermochimica acta

Melting transition of polyethylene studied by light-modulated calorimetry

Yasuo Saruyama*

Faculty of Textile Science, Kyoto Institute of Technology, Matsugasaki, Sakyoku, Kyoto 606, Japan

Received 6 August 1996; accepted 14 March 1997

Abstract

Melting transition of polyethylene crystals was studied by light-modulated calorimetry. The light-modulated calorimeter (or light-heating dynamic DSC) was constructed using heating through light to give heat-flow modulation to the sample. Frequency dependence of the complex heat capacity was measured in the (0.01–0.2) Hz range. It was found that, in the melting-temperatures range, the real part of the complex heat capacity at frequencies equal to or higher than 0.1 Hz reached limiting value at a sufficiently high frequency. Linearity between the cyclic temperature change of the sample and the modulation, and the difference between melting and crystallization from the viewpoint of the complex heat capacity were also investigated. © 1997 Elsevier Science B.V.

Keywords: Complex heat capacity; First-order phase transition; Light-modulated calorimetry; Polyethylene; Temperature modulated calorimetry

1. Introduction

Temperature-modulated calorimetry (TMC) is a recently developed technique of thermal analysis with modulation to generate cyclic temperature change of the sample. We constructed a TMC apparatus combining a light-heating system for the modulation with a commercial DSC apparatus [1,2]. Hereafter, our method of TMC will be called light-modulated calorimetry (LMC). One type of TMC apparatus generates the modulation by adding sinusoidal temperature profile to the linear heating/cooling of the conventional differential scanning calorimetry (DSC) [3,4]. TMC generates the conventional DSC signal superimposed with signal of the cyclic temperature change which, hereafter, will be called the cyclic component. The following two characteristic features of TMC have been established. Firstly, TMC provides a new technique of quantitative measurement of heat capacity with improved precision at slow scanning rates [5,6]. Secondly, TMC separates the contribution of heat absorption/emission accompanying an irreversible process on account of the contribution of the heat capacity [3,4]. The second feature has been successfully applied to analysis of the curing process of thermosetting resins [7].

On the other hand, the first-order phase transition, which is one of the important phenomena to be studied by thermal analysis, has not been studied extensively by TMC. It has been reported that a large phase shift was observed in the cyclic component at the melting temperature of a polymeric material [8]. However, useful information of the material undergoing phase

*Corresponding author. Fax: +81-75-724-7710; e-mail: saruyama@ipc.kit.ac.jp.

PII S0040-6031(97)00181-0

transition has not been obtained from the experimental data. Phase shift reflects dynamic properties of the material. As in the cases of dynamic mechanical and dielectric properties, it is important to study frequency dependence of the cyclic component at the phase-transition temperature.

It was pointed out that the cyclic component was nonlinear to modulation at the first-order phase-transition temperature of sodium nitrite ($NaNO_2$) [9] and at the melting temperature of indium [10]. Those materials have definite phase-transition temperatures. On the other hand, polymeric materials have wide distribution of phase-transition temperature. The width of the transition temperature range (> 1 K) is much larger than the amplitude of the cyclic temperature change of the sample in LMC (< 0.1 K). It is necessary to know whether or not the cyclic component is nonlinear to the modulation in the case of polymeric materials.

The layout of this paper is as follows. In Section 2, experimental conditions are described with an outline of our LMC apparatus. In Section 3, a calibration method to obtain the complex heat capacity from the cyclic component is explained. In Section 4, experimental results and discussions are given. The fourth section is composed of four subsections. In Section 5, concluding remarks are given.

2. Experimental

The sample material was polyethylene (NIST SRM1475, $M_w = 5.2 \times 10^4$, $M_w/M_n = 2.9$). The original pellets were melted and pressed between polytetrafluoroethylene films. The obtained film was cut and put into the aluminum pan. The sample was 0.1 mm thick and weighed 1.5 mg. The aluminum lid was put on the sample, then the sample was melted in a DSC furnace so as to spread out over the pan and the lid. The pan was not crimped to avoid deformation of the bottom. The bottom of the pan has to be flat to maintain good thermal contact between the bottom of the pan and the temperature detector. The upper surface of the lid was covered with carbon for light absorption. On the reference side, an aluminum pan with a lid attached to the bottom of the pan with a small amount of grease was used.

The LMC apparatus was constructed by combining light-heating system with a commercial DSC apparatus (heat-flux type, Rigaku DSC 8230) [1]. The light for the modulation was incident to both the sample and reference sides or only the sample side passing through glass windows made on the furnace covers. Intensity of the light was modulated by two polarizers; one was rotated by a stepping motor and the other remained fixed. Furnace temperature was controlled to change at a constant rate since the modulation was made by the light. The LMC apparatus was operated in one of two optional modes. The first mode was 'single-modulation mode' in which the modulated light was incident only at the sample side and light of constant intensity was incident at the reference side for temperature balance. The second mode was 'differential mode' in which the modulated light was incident at both the sample and reference sides.

Polyethylene and indium were measured in the single-modulation mode to observe temperature modulation of only the sample side at melting-transition temperature. The modulation frequency was 0.1 Hz and the heating rate of the furnace 0.4 K/min for polyethylene and 0.1 Hz and 1 K/h for indium. Higher harmonic components (0.2 and 0.3 Hz) together with 0.1 Hz component of the temperature modulation of polyethylene were calculated to check linearity between the cyclic heat flow and the temperature modulation. Other measurements were carried out in the differential mode to investigate detailed temperature dependence of the heat capacity. Temperature range from 312 to 440 K was scanned at the heating/cooling rate of 1 K/min and the modulation frequency of 0.1 Hz to compare the complex heat capacity on the heating and cooling processes. Frequency dependence of the complex heat capacity was studied at 0.01, 0.02, 0.05, 0.1 and 0.2 Hz over the (394–413) K temperature range at a heating rate of 0.1 K/min. A temperature range from 380 to 420 K was scanned at the heating rate of 1 K/min with the modulation frequency of 0.5 Hz to estimate the heat capacity of the crystal in the melting temperature range. Aluminum pans with two or three lids attached to the bottom of the pan with a small amount of grease were measured as standard materials. The standard materials were measured at every frequency used since the calibration constants were significantly dependent on the frequency. On the other hand, the

heating rate was fixed to 2 K/min since the calibration constants were not dependent on the heating rate.

3. Calibration method

A calibration method to obtain the complex heat capacity in the single-modulation mode has already been reported [2]. The basic equations of LMC for the cyclic component are

$$i\omega T_s C_s = Q_s - KT_s - (LT_s - MT_r) \quad (1)$$

and

$$i\omega T_r C_r = Q_r - KT_r - (LT_r - MT_s) \quad (2)$$

where ω is angular frequency of the modulation, T_s, C_s and Q_s the complex amplitudes of the cyclic component of temperature change on the sample side, heat capacity of the sample side and light energy flow to the sample side, respectively, KT_s the complex amplitude of heat outflow from the sample side to the furnace wall. The heat outflow does not depend on the furnace temperature because the furnace is not modulated in our LMC, and $(LT_s - MT_r)$ the complex amplitude of heat exchange between the sample and reference sides due to temperature difference between the sample and reference sides. If heat capacity of the material between the sample and reference sides is negligible L and M are real and equal to one another, and this term becomes Newton's law. Meaning of the symbols with subscript 'r' are similar to those with subscript 's'.

Using heat capacity difference C defined as $C = C_s - C_r$, the left-hand side of Eq. (1) becomes $i\omega T_s(C_r + C)$. Then Eqs. (1) and (2) can be solved, and T_s and T_r expressed in terms of C, ω, C_r, K, L, M, Q_s and Q_r. The temperature difference T is defined as $T = T_s - T_r$. T is given by the following equation:

$$T = \frac{(\alpha - M)Q_s + (-\alpha + M - i\omega C)Q_r}{-M^2 + (i\omega C + \alpha)\alpha} \quad (3)$$

where $\alpha = i\omega C_r + K + L$. Remembering that $Q_s = Q_r$ and $Q_r = 0$ correspond to the differential mode and the single-modulation mode, respectively, the following equations are obtained.

1. Differential mode

$$\frac{1}{T} = \frac{p}{C} + q \quad (4)$$

where $p = (M^2 - \alpha^2)/i\omega Q_s$ and $q = -\alpha/Q_s$.

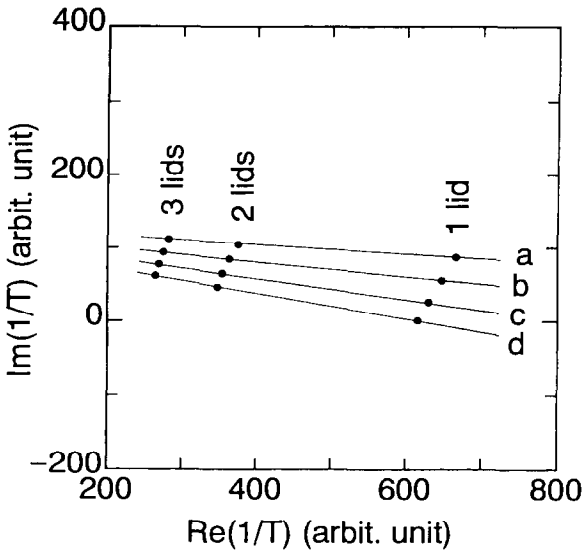

Fig. 1. $1/T$ of Eq. (4) plotted in the complex plane. The number of aluminum lids used as standard material is given in the figure. Lines a, b, c and d are the results at 330, 370, 410 and 450 K, respectively.

2. Single-modulation mode

$$\frac{1}{T} = p'C + q' \quad (5)$$

where $p' = i\omega\alpha/(\alpha - M)Q_s$ and $q' = (\alpha + M)/Q_s$, p, q, p' and q' are independent of C. In the case of Eqs. (4) and (5), points of $1/T$ plotted in the complex plane for various values of C should be on a line as long as C is real. Eq. (5) has already been reported and confirmed experimentally [2]. Experimental results of the differential mode at the modulation frequency of 0.1 Hz are shown in Fig. 1. Aluminum pans with one, two or three lids were used as standard materials. Lines a, b, c and d are the results at 330, 370, 410 and 450 K, respectively. At each temperature, the observed points are on a line. Distance between the points of one and two lids should be three times as long as that between the points of two and three lids. Observed value is 3.2 which shows validity of Eq. (4). After the values of p, q, p' and q' are determined using standard materials, complex values of heat capacity of the sample can be calculated from Eq. (4) or Eq. (5).

4. Results and discussion

4.1. Linearity of the cyclic component

Higher harmonics of the modulation frequency were investigated in the observed LMC signal around the melting temperatures of polyethylene (390.0–412.7 K). The results are shown in Fig. 2 in which amplitude of harmonic components are given. It is apparent that the 0.1 Hz component (the modulation frequency) exhibits anomalous behavior in the time range of melting, but the higher harmonic components stay zero in that time range. This result shows that higher harmonics of temperature response to the modulation are negligible in the case of polyethylene. This is in contrast to the results of sodium nitrite [9] and indium [10]. As shown in Fig. 2, the amplitude of the 0.1 Hz component is < 0.01 K. It should be remembered that the amplitude of the 0.1 Hz component is much smaller than the width of the melting temperature range of polyethylene crystals, which is much larger than 1 K. It can be assumed that, in the case of polymeric materials having wide distribution of the first-order phase transition temperatures, the cyclic temperature change is linear to the modulation. Amplitude of the cyclic component in the experiments of the following sections is ca. 0.1 K which is larger than the amplitude of Fig. 2 but still fits with the above-mentioned assumption.

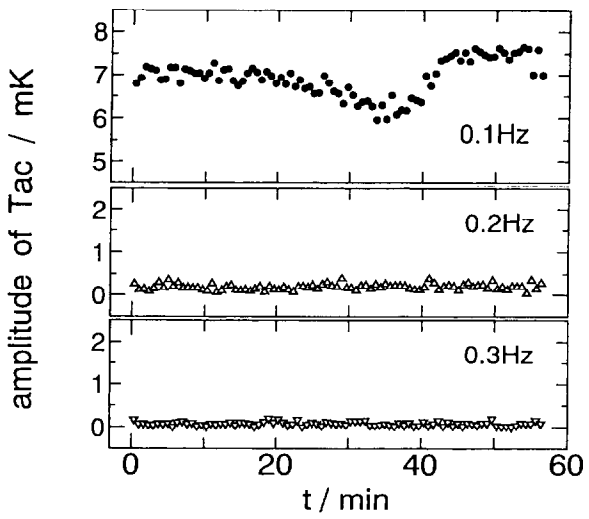

Fig. 2. Amplitude of first-, second- and third-harmonic components of the observed signal around the melting region of polyethylene crystals measured in the single-modulation mode. The modulation frequency is 0.1 Hz. The observed region in temperature scale is (390.5–412.7) K.

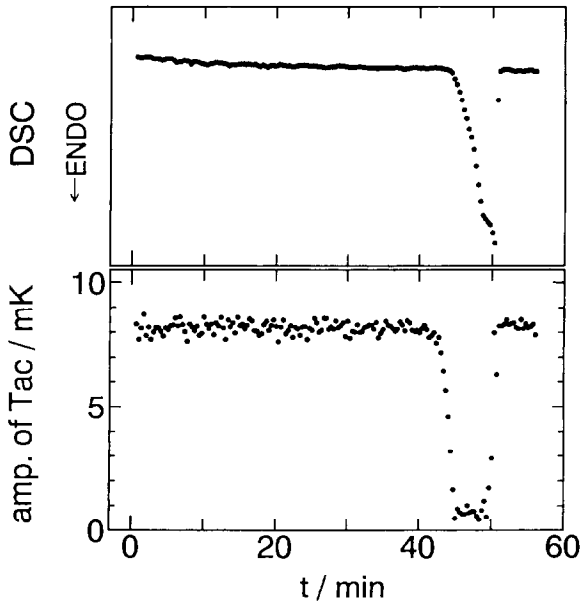

Fig. 3. Amplitude of the cyclic temperature change and DSC signal (total heat flow) of indium around the melting region measured in the single-modulation mode. The modulation frequency is 0.1 Hz. The observed region in temperature scale is (428.8–429.7) K.

Nonlinearity of indium [10] was reported on the basis of the behavior of the conventional DSC signal at the melting temperature. The cyclic-temperature change of indium around the melting temperature (428.8–429.7 K) was measured. The results are shown in Fig. 3. The time range of melting can be determined from the DSC signal (total heat flow). In the melting time range, the amplitude of the cyclic temperature change is very small. This small amplitude can be attributed to the fast phase transition of indium, that is, indium can reach the equilibrium state at the melting temperature rapidly enough to follow the modulation. The temperature response to the modulation may be nonlinear, but actually the resultant signal is too small to be detected.

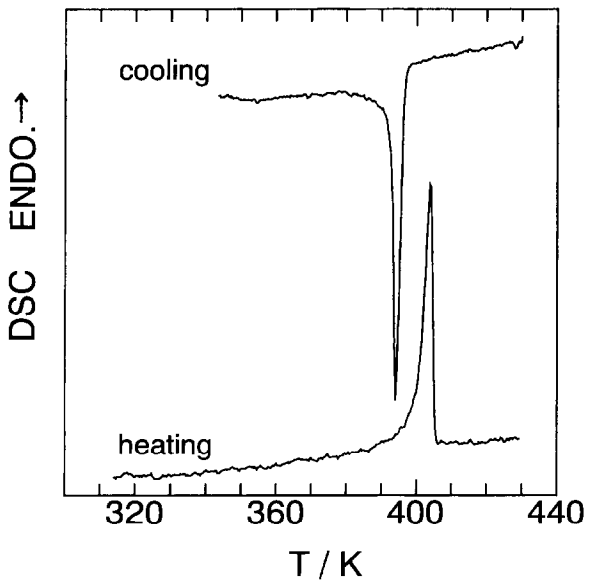

Fig. 4. DSC signal (total heat flow) of polyethylene on heating and cooling processes.

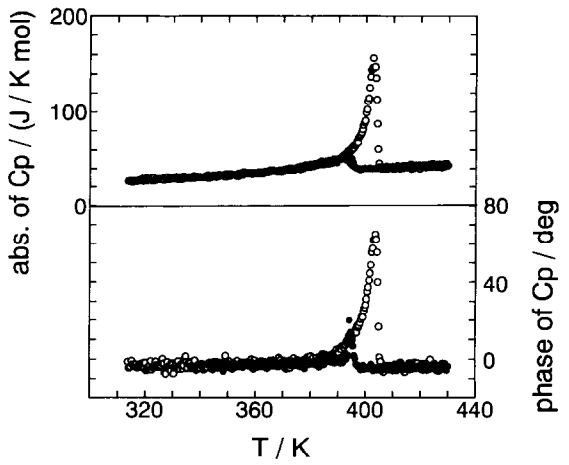

Fig. 5. Complex heat capacity of polyethylene. The upper and lower curves are the amplitude and the phase, respectively. The modulation frequency is 0.1 Hz. The open and solid circles show heating and cooling processes, respectively.

4.2. *Comparison between the heating and cooling processes*

Results of LMC of polyethylene between 312 and 430 K are shown in Figs. 4 and 5, which reproduce the DSC signal (total heat flow) and the complex heat capacity, respectively. The modulation frequency was 0.1 Hz and the heating/cooling rate of the furnace 1 K/min. Absolute value of the complex heat capacity at 410 K, when phase of the complex heat capacity is very close to zero, is 15% greater than the literature value of amorphous polyethylene [11]. This disagreement is considered to be due to insufficient evaluation of the constants p and q in Eq. (4). However, qualitative results will not be changed if more precise value of p and q are used.

In Fig. 5, the absolute value and the phase of the complex heat capacity have peaks on both the heating and cooling processes. These peaks are attributed to the phase transitions of polyethylene since the peak temperatures agree well with those of DSC signal in Fig. 4. It should be noted that melting and crystallization appear distinct phenomena from the viewpoint of complex heat capacity. During the cooling process, the phase exhibits a small anomaly at the crystallization temperatures. On the other hand, during the heating process both the amplitude and the phase have large peaks in the melting temperature range. This difference between the heating and cooling processes can be attributed to the difference of coupling strength between the modulation and the phase transition. Since crystallization occurs at a large supercooling, the rate of crystallization is little affected by the small temperature modulation, i.e. the coupling between the crystallization and the modulation is weak. On the other hand, the melting occurs at a small superheating where the rate of phase transition is sensitive to temperature change, i.e. the coupling between the melting and the modulation is strong. As the coupling becomes weaker, contribution of the phase transition to the complex heat capacity becomes smaller. If the rate of phase transition is independent of the modulation, the complex heat capacity will not show anomaly during the phase transition as seen in the case of cold crystallization of polyethylene terephthalate [3,4].

It will be reported in the near future that linear approximation for modulation dependence of the crystallization rate holds because of the weak coupling and useful information of crystallization rate can be obtained from the phase shift of the complex heat capacity. On the other hand, the coupling behavior on the heating process is too complicated to be fully analyzed at present. As the first step of investigation

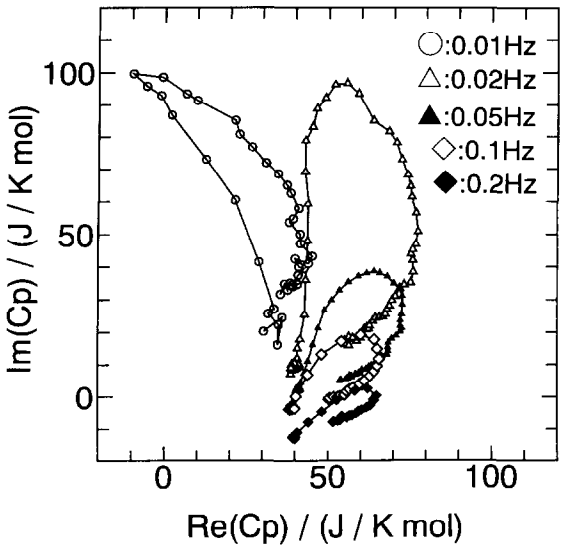

Fig. 6. Frequency dependence of the complex heat capacity. The horizontal and vertical axes show the real and imaginary parts, respectively. Measured temperature range is between 394 and 413 K. Observed point moves counterclockwise along each curve as temperature increases. Frequencies are given in the graph.

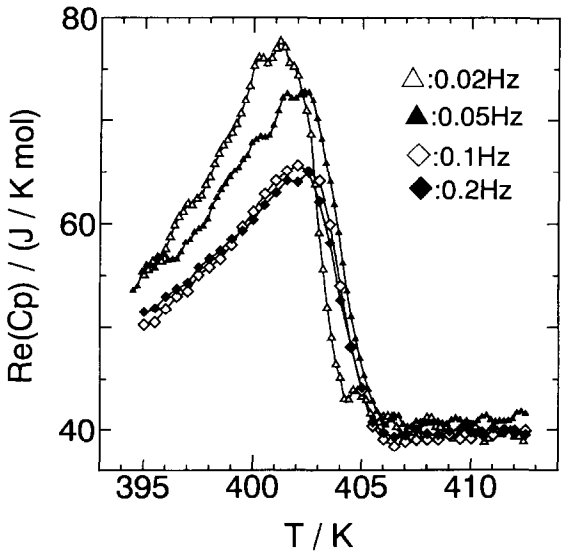

Fig. 7. Temperature dependence of the real part of the complex heat capacities at different frequencies given in the graph.

of the melting transition, the frequency dependence of the complex heat capacity was studied.

4.3. Frequency dependence

Fig. 6 shows frequency dependence of the complex heat capacity. The horizontal and vertical axes show real and imaginary parts of the complex heat capacity, respectively. Each frequency covers the temperature range from 394 to 413 K and the observed point moves counterclockwise along the curve as the temperature rises. Phase shift is zero when the imaginary part is zero. Fig. 6 shows that the phase shift becomes significantly larger as the frequency becomes smaller. At 0.01 Hz the phase shift exceeds $\pi/2$ radians. The amount of phase shift has to be smaller than $\pi/2$ radians according to theoretical studies of the complex heat capacity [12–14]. The result of 0.02 Hz exhibits a slight shift to the left of the graph around the top of the curve. These results suggest that the observed data at frequencies equal to or lower than 0.02 Hz are difficult to be explained sufficiently. The observed imaginary part is not always zero in the melt in which there is no thermal anomaly. This is due to insufficient evaluation of the constants p and q in Eq. (4). However, the foregoing discussion will not be changed if more precise values of p and q are used.

According to the theoretical studies [12–14], the imaginary part is zero and the real part is independent of the frequency at sufficiently high frequencies. The real parts of 0.1 and 0.2 Hz seem to agree with each other. Fig. 7 shows that the agreement of 0.1 and 0.2 Hz is fairly good. We assume that the real part of the frequencies, equal to or higher than 0.1 Hz, is identical with the limiting value at a sufficiently high frequency although the imaginary part has not yet reached zero.

4.4. Heat capacity of the polyethylene crystal in the melting temperature range

Heat capacity of the crystal in the melting-temperature range during the heating process was calculated. The fraction of the amorphous phase at temperature T was written as $x(T)$. Increase of $x(T)$ between 385 and 415 K was specially studied since the phase shift of the complex heat capacity was very small outside of this temperature range, as shown in Fig. 5. We define x' by the following equation:

$$x'(T) = \frac{x(T) - x_{(385\,\mathrm{K})}}{1 - x_{(385\,\mathrm{K})}} \tag{6}$$

The numerator and denominator of the right-hand side represent the increase of the amorphous fraction (decrease of crystal fraction) between 385 and T K, and the crystal fraction at 385 K, respectively. The value of x' at temperature T was estimated using the following equation:

$$x' = \frac{\int_{385\,K}^{T}(C_{DSC} - C_{cyc})dT}{\int_{385\,K}^{415\,K}(C_{DSC} - C_{cyc})dT} \quad (7)$$

where C_{DSC} and C_{cyc} are the heat capacities obtained from the DSC signal and the real part of the cyclic component, respectively. The value of C_{cyc}, obtained at the modulation frequency of 0.5 Hz, was used. C_{cyc} at 0.5 Hz is equal to the limiting value at a sufficiently high frequency as already mentioned. Since the difference between C_{DSC} and C_{cyc} is attributed to the phase transition, $(C_{DSC} - C_{cyc})$ at temperature T is proportional to the number of the crystals having the melting point at temperature T.

C_{DSC} was obtained by the following method. The observed DSC signal and DSC signal, which should have been obtained if the heat capacities of the sample and reference sides were equal to one another, were written as D_{obs} and D_0, respectively. C_{DSC} was expressed as:

$$C_{DSC} = s(D_{obs} - D_0) \quad (8)$$

where s is a scale factor. We assumed that D_0 was linear in temperature.

$$D_0 = tT + u \quad (9)$$

Substituting Eq. (9) in Eq. (8), we obtained:

$$C_{DSC} = s(D_{obs} - tT - u) \quad (10)$$

Values of three parameters s, t and u in Eq. (10) were determined from the following three conditions:

1. C_{DSC} (385 K) = C_{cyc} (385 K)
2. C_{DSC} (415 K) = C_{cyc} (415 K)
3. The denominator of Eq. (7) is equal to the total value of the latent heat.

Values of the right-hand side of the first and second conditions were experimentally obtained. Crystallinity of the measured sample at 385 K, $(1 - x_{(385\,K)})$, which was necessary to determine the total value of the latent heat, was not measured. We calculated x' with s, t and u, estimated in two extreme cases: $(1 - x_{(385\,K)}) = 1$ and $(1 - x_{(385\,K)}) = 0.5$. The value of the latent heat per mole obtained by Gaur and Wunderlich [11] was used. Fig. 8 shows temperature dependence of x', calculated in the case of $(1 - x_{(385\,K)}) = 1$. Maximum difference between the two x' values, corresponding to $(1 - x_{(385\,K)}) = 1$ and $(1 - x_{(385\,K)}) = 0.5$ was less than 0.03. Therefore, the x' values calculated in the case of $(1 - x_{(385\,K)}) = 1$ were used in the following calculations.

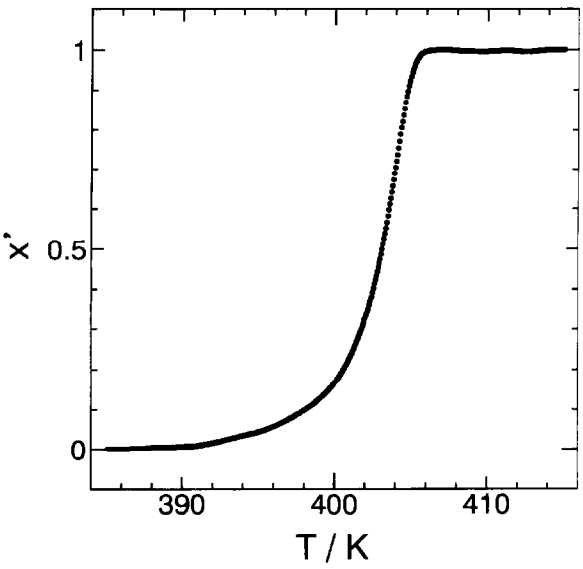

Fig. 8. Temperature dependence of x' defined by Eq. (7). Crystallinity at 385 K was assumed to be 100%. x' in the case of 50% crystallinity was also calculated but the maximum deviation from this graph was less than 0.03.

It was assumed that C_{cyc} was equal to weighted average of heat capacities of the crystal and the amorphous sample:

$$C_{cyc} = (1 - x)C_c + xC_a \quad (11)$$

where C_x and C_a were the heat capacities of 100% crystalline and 100% amorphous samples, respectively. From Eq. (11) we obtained

$$C_c = \frac{C_{cyc} - C_a}{1 - x} - C_a \quad (12)$$

From Eq. (6)

$$1 - x = (1 - x_{(385\,K)})(1 - x') \quad (13)$$

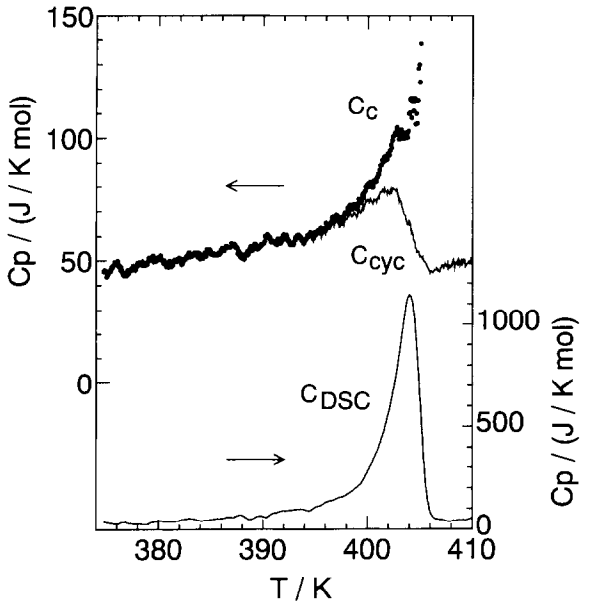

Fig. 9. Temperature dependence of calculated heat capacity of the crystal in the melting-temperature range together with observed heat capacities from the cyclic component and the DSC data. The modulation frequency is 0.5 Hz. Crystallinity at 385 K was assumed to be 100% in the calculation.

Substituting Eq. (13) in Eq. (12)

$$C_c = \frac{1}{1 - x_{(385\,K)}} \frac{C_{cyc} - C_a}{1 - x'} + C_a \qquad (14)$$

Eq. (14) shows that C_c increases as the crystallinity at 385 K becomes decreases. We calculated the values of C_c in the case of $(1 - x_{(385\,K)}) = 1$ which gave the minimum of C_c. The values of C_a were obtained by linear extrapolation from temperatures higher than 415 K. The results are shown in Fig. 9 together with C_{cyc} and C_{DSC}. C_c distinctively increases in the melting-temperature range. Such a behavior suggests that the melting of polyethylene crystal is, at least in part, of a cooperative nature. C_c might contain contribution of fast process of melting transition, but estimation of such a contribution has to be left for future works.

5. Conclusion

Melting transition of polyethylene was studied with LMC. We found that LMC is an effective technique to study the first-order phase transitions of polymeric materials. The cyclic temperature change was linear to the modulation at the frequency of 0.1 Hz in the case of polyethylene. This will be correct in the case of other polymers which have wide distribution of the first-order phase-transition temperature. Comparing the heating and cooling processes, we found that melting and crystallization appeared to be quite different phenomena from the viewpoint of the complex heat capacity. We found that the real part of the complex heat capacity at frequencies equal to or higher than 0.1 Hz is equal to the limit value corresponding to the result at a sufficiently high frequency. Using the limiting value, we calculated heat capacity of the crystal in the melting-temperature range. Cooperative nature of the melting was suggested.

It should be noted that frequency dependence should be measured to study the first-order phase transitions. It is necessary to find the threshold value of the modulation frequency to give the limiting value of the complex heat capacity.

References

[1] M. Nishikawa and Y. Saruyama, Thermochim. Acta, 267 (1995) 75.
[2] Y. Saruyama, Thermochim. Acta, 282/283 (1996) 157.
[3] P.S. Gill, S.R. Sauerbrunn and M. Reading, J. Therm. Anal., 40 (1993) 931.
[4] M. Reading, D. Elliott and V.L. Hill, J. Therm. Anal., 40 (1993) 949.
[5] B. Wunderlich, Y. Jin and A. Boller, Thermochim. Acta, 238 (1994) 277.
[6] A. Boller, Y. Jin and B. Wunderlich, J. Therm. Anal., 42 (1994) 307.
[7] G. Van Assche, A. Van Hemelrijck, H. Rahier and B. Van Mele, Thermochim. Acta, 268 (1995) 121.
[8] M. Reading, A. Luget and R. Wilson, Thermochim. Acta, 238 (1994) 295.
[9] I. Hatta, H. Ichikawa and M. Todoki, Thermochim. Acta, 267 (1995) 83.
[10] T. Ozawa and K. Kanari, Thermochim. Acta, 253 (1995) 183.
[11] U. Gaur and B. Wunderlich, J. Phys. Chem. Ref. Data, 10 (1981) 119.
[12] A. Toda, T. Oda, M. Hikosaka and Y. Saruyama, Polymer, 38 (1997) 231.
[13] A. Toda, T. Oda, M. Hikosaka and Y. Saruyama, Thermochim. Acta, in press.
[14] N.O. Birge, Phys. Rev., B34 (1986) 1631.